

# Ion Permeation by a Folded Multiblock Amphiphilic Oligomer Achieved by Hierarchical Construction of Self-Assembled Nanopores

Takahiro Muraoka,<sup>\*,†</sup> Tatsuya Shima,<sup>†</sup> Tsutomu Hamada,<sup>‡</sup> Masamune Morita,<sup>‡</sup> Masahiro Takagi,<sup>‡</sup> Kazuhito V. Tabata,<sup>§</sup> Hiroyuki Noji,<sup>§</sup> and Kazushi Kinbara<sup>\*,†</sup>

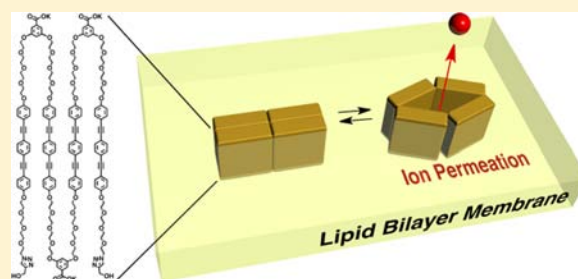
<sup>†</sup>Institute of Multidisciplinary Research for Advanced Materials, Tohoku University, 2-1-1, Katahira, Aoba-ku, Sendai 980-8577, Japan

<sup>‡</sup>School of Materials Science, Japan Advanced Institute of Science and Technology, 1-1, Asahidai, Nomi, Ishikawa 923-1292, Japan

<sup>§</sup>Department of Applied Chemistry, School of Engineering, The University of Tokyo, Bunkyo-ku, Tokyo 113-8656, Japan

## Supporting Information

**ABSTRACT:** A multiblock amphiphilic molecule **1**, with a tetrameric alternating sequence of hydrophilic and hydrophobic units, adopts a folded structure in a liposomal membrane like a multipass transmembrane protein, and is able to transport alkali metal cations through the membrane. Hill's analysis and conductance measurements, analyzed by the Hille equation, revealed that the tetrameric assembly of **1** forms a 0.53 nm channel allowing for permeation of cations. Since neither **3**, bearing flexible hydrophobic units and forming no stacked structures in the membrane, nor **2**, a monomeric version of **1**, is able to transport cations, the folded conformation of **1** in the membrane is likely essential for realizing its function. Thus, function and hierarchically formed higher-order structures of **1**, is strongly correlated with each other like proteins and other biological macromolecules.



## INTRODUCTION

Membrane transport of solutes such as ions and small molecules is an important cell function to maintain viability.<sup>1</sup> Channel proteins play major roles in this activity to regulate metabolism, signal transduction, osmolyte homeostasis, and waste removal. The transport activities as well as the unique structures of channel proteins have caught the interests of chemists and have compelled them to develop numerous synthetic channels,<sup>2</sup> allowing permeation of protons,<sup>3,4</sup> ions,<sup>5–7</sup> and small organic molecules<sup>8–10</sup> through a lipid bilayer membrane. Likewise, construction of channels by a fully synthetic approach allows for exploring the mechanisms of channel proteins<sup>11</sup> and furnishing lipid and cellular membranes with artificial functions.<sup>12</sup>

Typical architectures of the synthetic channels can be classified into two models, namely, toroidal<sup>3,5,8,11a</sup> and barrel-stave models.<sup>4,6,9</sup> Crown ethers,<sup>5c,d,f,8a,b,11a</sup> cyclodextrins,<sup>5g</sup> cyclic peptides,<sup>5b,e</sup> and aromatic macrocycles<sup>3,5a</sup> have been used in the former models as cyclic components for stacking, while rigid rod-shaped molecules have been applied to construct the barrel-stave channels. These are mostly supramolecular architectures, where controlled assembly of such preorganized molecules or molecular components enables construction of nano- or subnano-sized channels. In contrast to such design strategy of the artificial channels, nature makes use of folding linear molecules as a means to construct channels in order to realize membrane transportation functions. Namely, while the channel proteins are intrinsically made of a linear peptide chain, they develop the building blocks that intra-

molecularly assemble with each other in appropriate geometries for constructing the channels, through folding the peptide chain into secondary structures such as  $\alpha$ -helices and  $\beta$ -sheets.<sup>13</sup>

Recently, we have developed multiblock linear amphiphiles such as **1** and **2** (Figure 1) composed of alternately arranged hydrophilic and hydrophobic units. These molecules are designed to mimic the structural feature of multipass transmembrane (MTM) proteins, and actually, **1** adopts a folded conformation<sup>14</sup> in a liposomal membrane like MTM proteins through the intramolecular  $\pi$ - $\pi$  stacking of the hydrophobic aromatic units.<sup>15</sup> Here we report that the multiblock amphiphile **1**, folded in the membrane, is capable of transporting ions via the channel formation through self-assembly. The hierarchically constructed supramolecular assembly, formed after folding of the linear molecule **1**, corresponds to the quaternary structure of protein and is essential for realization of the ion permeation.

## RESULTS AND DISCUSSION

**Location and Orientation of the Multiblock Amphiphiles **1** and **2** in Phospholipid Bilayers.** In our previous study, we reported a series of multiblock amphiphiles, such as **1** and **2** (Figure 1), composed of alternately arranged hydrophilic and hydrophobic units with different numbers of the repeating units.<sup>15</sup> These molecules bear fluorescent 1,4-bis(4-phenylethynyl)benzene (BPEB)<sup>16</sup> moieties as the hydro-

Received: August 28, 2012

Published: November 12, 2012

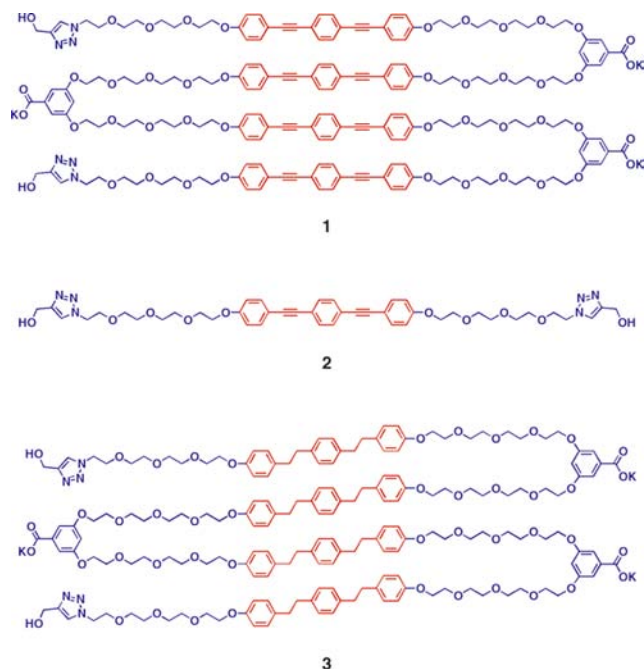


**Figure 1.** Multiblock amphiphilic molecules **1**, **2**, and **3** with an alternately arranged hydrophobic (red) and hydrophilic (blue) units.

phobic units that are connected with hydrophilic tetraethylene glycol (TEG) and benzoate groups. Phase-contrast and fluorescent optical microscope studies revealed that **1** and **2** locate at the bilayer membrane of giant unilamellar vesicles (GUVs) formed with 1,2-dioleoyl-*sn*-glycero-3-phosphocholine (DOPC).<sup>17</sup> On the basis of the fluorescence profile at the various concentrations as well as the absorption spectroscopic analyses, it is most likely that **1** adopts a folded conformation in the liposomal membrane, like multipass transmembrane (MTM) proteins, by forming intramolecular H-stacking of the hydrophobic units. At relatively high concentrations, **1** showed a propensity to form an intermolecular assembly. In contrast, compound **2**, a monomeric version of **1**, forms intermolecular self-assembly in a membrane according to the increase of its concentration.<sup>15</sup>

At first, the location and orientation of **1** and **2** in a liposomal membrane were studied by a fluorescence depth quenching method.<sup>18</sup> We used the following three spin-labeled phospholipids: 1-palmitoyl-2-stearoyl-(5-doxyl)-*sn*-glycero-3-phosphocholine (5-doxyl PC), 1-palmitoyl-2-stearoyl-(12-doxyl)-*sn*-glycero-3-phosphocholine (12-doxyl PC), and 1-palmitoyl-2-stearoyl-(16-doxyl)-*sn*-glycero-3-phosphocholine (16-doxyl PC), bearing spin probes at different positions in the alkyl tails. GUVs of DOPC including **1**, **2**, and these spin-labeled phospholipids have been prepared according to the reported procedure.<sup>15</sup> Since efficiency of fluorescence quenching depends on the distance between the spin probe and a chromophore, the location and orientation of the BPEB units of **1** and **2** could be investigated by using these spin-labeled phospholipids.<sup>19</sup> Actually, incorporation of 5-doxyl PC into DOPC GUVs including **1** (GUVs•**1**) resulted in a 31% decrease of the fluorescence intensity of **1** (Figure 2a; [DOPC] + [doxyl PC] = [total PC] = 0.20 mM, [DOPC]/[doxyl PC] = 90/10, [1]/[total PC] = 0.00050, 20 mM HEPES, 50 mM KCl, pH 7.1, 20 °C). On the other hand, 12- and 16-doxyl PCs comparably quenched the fluorescence of **1** (44% and 43%, respectively) with efficiency higher than that of 5-doxyl PC

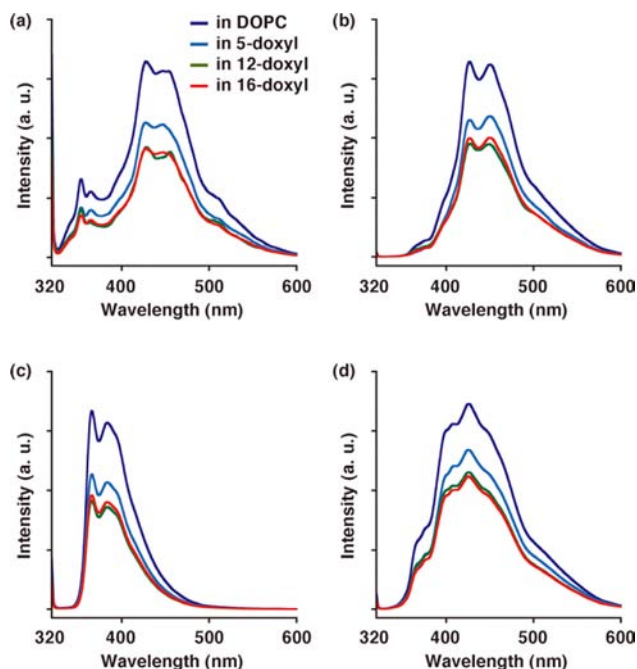


**Figure 2.** Fluorescence spectra of GUVs containing **1** at the ratio of [1]/[total PC] = (a) 0.00050 and (b) 0.10 and **2** at the ratio of [2]/[total PC] = (c) 0.00050 and (d) 0.10 with excitation at 315 nm ([total PC] = 0.20 mM, 20 mM HEPES, 50 mM KCl, pH 7.1, 20 °C). As membrane constituents, DOPC (blue line) and DOPC containing 10 mol % of 5-doxyl PC (sky blue line), 12-doxyl PC (green line), or 16-doxyl PC (red line) were used.

(Figure 2a). This trend was preserved upon increasing the concentration of **1**, encouraging intermolecular self-assembly (Figure 2b). Likewise, 12-doxyl PC and 16-doxyl PC showed quenching efficiency higher than that of 5-doxyl PC for GUVs•**2** (c and d of Figure 2). Thus, it is likely that the BPEB units of **1** and **2** locate not on the surface but preferentially in the middle of the lipid bilayer with mostly parallel orientation with DOPC molecules.

**Optical Microscopy of Giant Unilamellar Vesicles under Osmotic Pressure.** As a function of multiblock molecule **1** folded in a membrane, we have focused on ion permeation ability, since many MTM proteins have such functions in relation to signal transduction and active transport. Giant vesicles allow us to observe such transportation events by optical microscopy, where the osmotic pressure gradient induces deformation of liposomes with membrane fluctuation.<sup>20</sup> Upon addition of NaCl to a suspension of DOPC GUVs in 0.20 M sucrose aq at 20 °C, GUVs immediately displayed membrane fluctuation ([NaCl] = 2.5 mM, [DOPC] = 0.10 mM, 0.20 M sucrose; video 002.qt in the Supporting Information). This indicates that the liposomal membrane was kept under exposure to osmotic pressure due to the difference in the concentration of NaCl between the inside and outside of a GUV. In other words, a DOPC membrane is impermeable to the ions.<sup>21</sup> DOPC GUVs involving **2** in the membrane (GUV•**2**, [DOPC] = 0.10 mM, [2]/[DOPC] = 0.10) showed similar responses to the addition of NaCl ([NaCl] = 2.5 mM, 0.20 M sucrose aq, 20 °C; Figure 3a, video 003.qt in the Supporting Information). In sharp contrast, GUV•**1** ([DOPC] = 0.10 mM, [1]/[DOPC] = 0.025) stayed without fluctuation under identical conditions ([NaCl] = 2.5 mM, 0.20 M sucrose aq, 20 °C; Figure 3b, video 004.qt in the

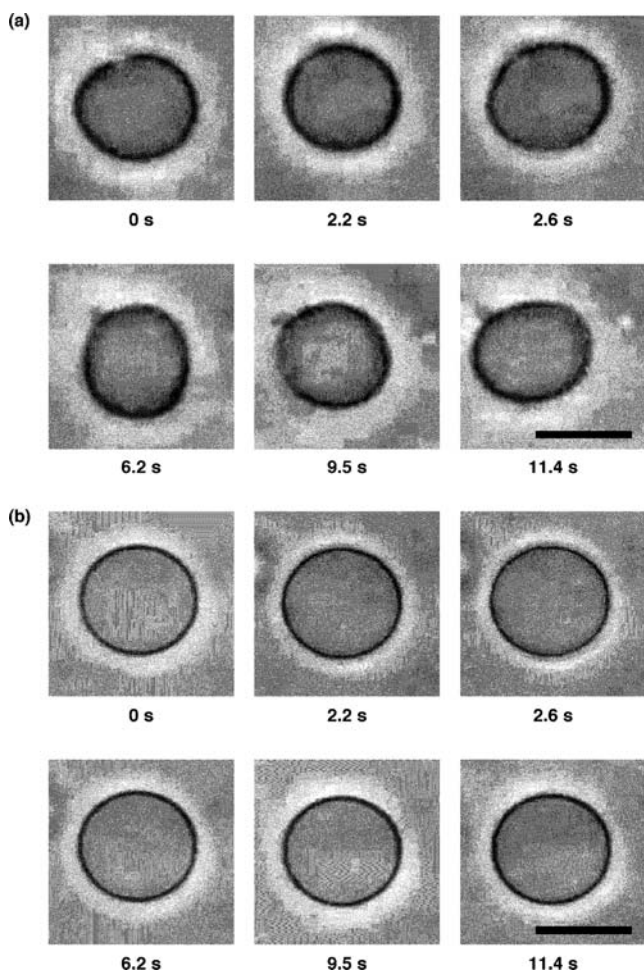


**Figure 3.** Phase contrast micrographs of DOPC GUVs ( $[DOPC] = 0.10$  mM) containing (a) 2 ( $[2]/[DOPC] = 0.10$ ) and (b) 1 ( $[1]/[DOPC] = 0.025$ ) in 0.20 M sucrose aqueous solution under exposure to osmotic pressure (2.5 mM NaCl). The observations began within 5 s after the addition of NaCl. The micrographs were taken at 0.3, 2.2, 2.6, 6.2, 9.5, and 11.4 s after initiation of the observation. The contrast of each image is adjusted for clarification. The scale bars represent 10  $\mu\text{m}$ . See also videos 002.qt–004.qt in the Supporting Information.

Supporting Information) for longer than 1 h. It should be noted that the fluctuation is not suppressed by altered membrane stiffness caused by incorporation of 2. The bending elastic modulus,  $B$ ,<sup>22</sup> of GUVs•2 was  $B_{GUVs\bullet 2} = 3.4 \times 10^{-20}$  J, which is smaller than that of DOPC GUVs ( $B_{GUVs} = 9.0 \times 10^{-20}$  J), indicating that the liposomal membrane of GUVs•2 is rather more flexible than that without 2.<sup>23</sup> Thus, the observed ion permeation event is likely due to 1 adopting the MTM-like folded conformation in the membrane similar to that of an ion channel of a membrane protein.

**Ion Transport Activities of the Multiblock Amphiphiles Investigated by Conductivity Measurements.** In order to investigate the ion transport activity of 1, a mixture of DOPC (12.7 mM) and 1 or 2 in *n*-decane was painted on an orifice ( $d = 150$   $\mu\text{m}$ ), which was sandwiched by two chambers containing HEPES buffer (20 mM HEPES, 50 mM KCl, pH 7.5, 0.30 mL each), where currents were recorded as a function of time at 20  $^{\circ}\text{C}$ . The planar DOPC bilayer membrane including 1 (10 nM) exhibited continuous currents of  $15.6 \pm 0.6$  pA in response to the applied voltage of +50 mV, displaying the existence of ion flow (Figure S1a in the Supporting

Information). It is important to note that upon decrease in the concentration of 1 down to 1.0 pM, the current became discontinuous with the mean lifetime of each current signal,  $\tau = 2.6$  ms (Figure 4). Generally, ion transport by a flip–flop

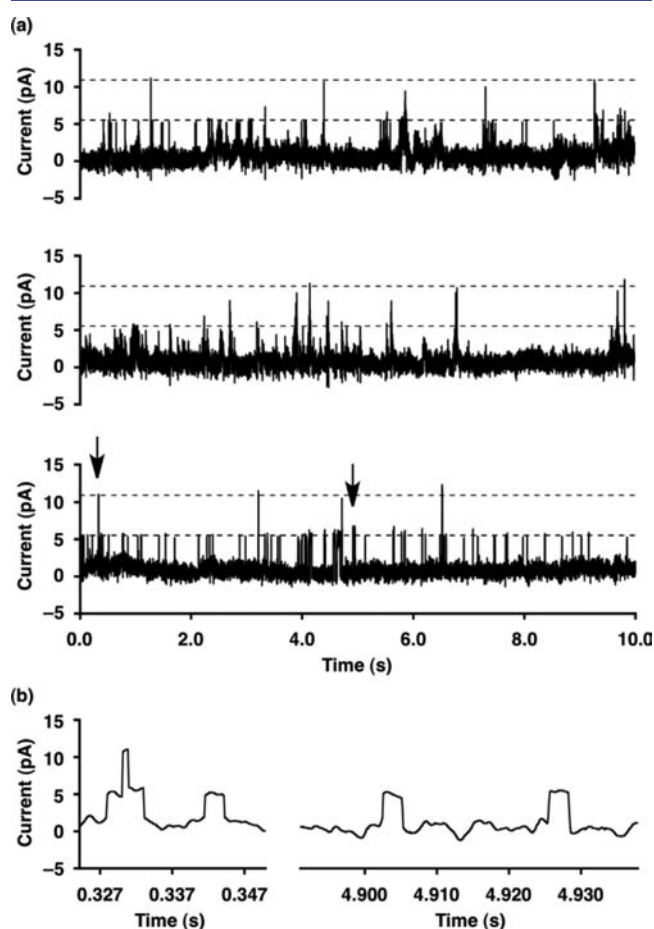


**Figure 4.** (a) Three independent conductance recordings of a DOPC liposomal membrane containing 1 (1.0 pM) at the applied voltage of +80 mV in HEPES buffer (20 mM, containing 50 mM KCl, pH 7.5) at 20  $^{\circ}\text{C}$ . (b) Enlarged views of the conductance recordings at the time periods denoted by arrows in (a).

mechanism takes place in a time scale of minutes to hours.<sup>24,25</sup> Therefore, the discontinuous current-flowing profile on the millisecond time scale dynamics strongly suggests that ions are transported not by a flip–flop mechanism but by permeation through a channel constructed by a dynamic assembly of multiple molecules of 1 embedded in the membrane. Interestingly, the observed currents were  $5.6 \pm 0.5$  pA or nearly twice as large as the value at the applied voltage of +80 mV ( $10.4 \pm 0.9$  pA). Taking into consideration the low concentration of 1<sup>26</sup> in the membrane, the former value is likely to correspond to one ion channel, while the latter corresponds to two channels that happened to be opened simultaneously. The current flow through the single channel revealed a linear correlation with the applied voltage (Figure 5). The inclination of this ohmic  $I$ – $V$  profile allows evaluation of the conductance of the transporter as  $g = 70$  pS.

**Ion Transport Activities of the Multiblock Amphiphiles Investigated by Fluorescence Measurements.** The ion transportation activity of 1 was further investigated using DOPC large unilamellar vesicles (LUVs,  $[DOPC] = 0.10$  mM)

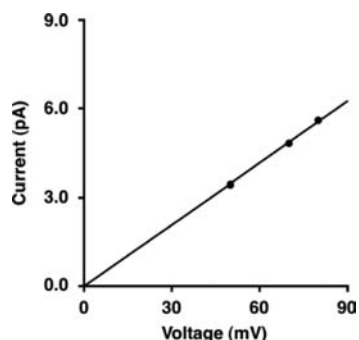


**Figure 5.** Single channel  $I$ - $V$  profile of a planar DOPC bilayer membrane ( $[DOPC] = 12.7$  mM) containing **1** (1.0 pM) in HEPES buffer (20 mM, containing 50 mM KCl, pH 7.5) at 20 °C.

loaded with 8-hydroxypyrene-1,3,6-trisulfonate (HPTS, 30  $\mu$ M). HPTS emits 510-nm fluorescence upon excitation with 450-nm light at pH higher than 5, and the fluorescence intensity increases upon enhancement of pH.<sup>27</sup> Successful preparation of the LUVs including **1** and **2** was confirmed by dynamic light-scattering (DLS) measurements showing the presence of 100-nm size particles for each sample (Figure 6).

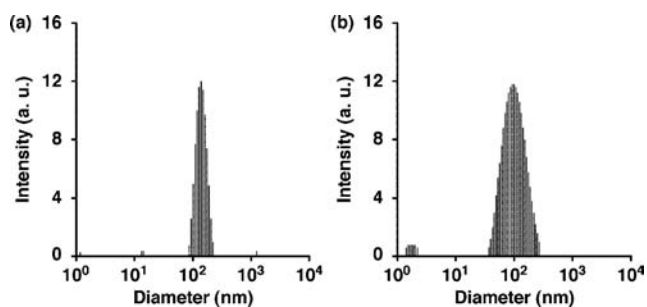


**Figure 6.** DLS profiles of DOPC-LUV ( $[DOPC] = 40$   $\mu$ M) containing (a) **1** (0.48  $\mu$ M) and (b) **2** (1.9  $\mu$ M) in 20 mM HEPES containing 50 mM KCl (pH 7.1) at 25 °C.

To the suspension of HPTS-loaded LUVs with embedded **1** (LUVs•**1**∩HPTS,  $[1]/[DOPC] = 0.012$ ) in 20 mM HEPES buffer containing 50 mM KCl at pH 7.1, was added an aqueous solution of NaOH at 20 °C ( $\Delta$ pH = 0.8). Immediately, fluorescence intensity at 510 nm was significantly enhanced, indicating that Na<sup>+</sup> permeates into LUVs•**1**∩HPTS (Figure 7a) to allow for the increase of pH inside the LUVs. Interestingly, addition of LiOH caused a faster increase in fluorescence intensity, while the addition of larger cations resulted in a slower increase compared with addition of NaOH. Provided that the cation permeation can be regarded as a first-order reaction, the relative rate constants are evaluated as follows:  $k_{Na}/k_{Li} = 0.57$ ,  $k_K/k_{Li} = 0.29$ ,  $k_{Rb}/k_{Li} = 0.11$  and  $k_{Cs}/k_{Li} = 0.043$ . This trend fits well with Eisenman sequence XI.<sup>28</sup> The Eisenman theory of ion permeability accounts for a balance of dehydration energy of a cation and cation binding energy in a transporter. Sequence XI indicates that the cation selectivity of **1** is mainly determined by the binding energy between the cation and **1**, suggesting that the BPEB units of **1** allow for cation- $\pi$  interaction, which is likely the major driving force for the permeation of these ions.<sup>29</sup>

The concentration dependency of the cation transportation rate of **1** was nonlinear as shown in Figure 7d. Curve fitting analysis based on the Hill equation<sup>30</sup> gave a Hill coefficient of  $n$

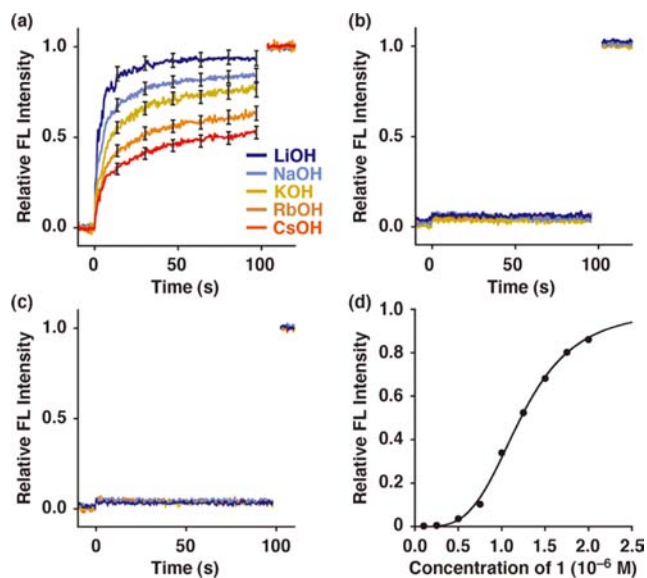


**Figure 7.** Changes in fluorescence intensity of HPTS entrapped in LUVs containing (a) **1** ( $[1]/[DOPC] = 0.012$ ), (b) **2** ( $[2]/[DOPC] = 0.048$ ), and (c) **3** ( $[3]/[DOPC] = 0.012$ ) in 20 mM HEPES containing 50 mM KCl (pH 7.1) at 20 °C (excitation at 460 nm, emission at 510 nm) as a function of time after the addition of an alkali metal hydroxide (LiOH, NaOH, KOH, RbOH, or CsOH) at 0 s followed by 1% triton X-100 at 100 s.  $\Delta$ pH = 0.8 (7.1 to 7.9). (d) Concentration dependency of the relative 510-nm fluorescence intensity of HPTS entrapped in LUVs containing **1** at 3.0 s after the addition of NaOH in 20 mM HEPES at 20 °C. Data are means ( $\pm$ standard deviations for (a) at every 16 s for clarity) of three independent experiments.

$= 3.8 \pm 0.1$ , indicating that the working channel is a tetramer (or, less likely, an octamer) of **1**.

**Ion Transport Activities of 2 and 3.** On the basis of the fluorescence depth quenching study, the BPEB unit of **2**, a monomeric version of **1**, is thought likely to locate at the middle of the liposomal membrane with a vertical orientation like that of **1**. However, in sharp contrast to **1**, the DOPC bilayer membrane containing **2** (10 nM or 1.0 pM) in the Supporting Information). In consistency, addition of alkali hydroxides to LUVs•**2**∩HPTS ( $[2]/[DOPC] = 0.048$ ) hardly caused enhancement of the fluorescence from HPTS (Figure 7b), even when the concentration of the BPEB units embedded in the membrane was the same as that of LUVs•**1**∩HPTS in Figure 7a. Since this concentration is high enough to induce self-assembly of **2**,<sup>15</sup> it is thought that ion permeation could not be realized merely by intermolecular stacking of BPEB units in the membrane. It should also be noted that **3**, obtained by hydrogenation of the ethynyl groups of **1** (Figure 1), also exhibited no ion transportation activity (Figure 7c, LUVs•**3**∩HPTS,  $[3]/[DOPC] = 0.012$ ). From all these results, intramolecular H-aggregation of the BPEB units of **1** to form a panel-like folded structure in the liposomal membrane is likely essential for developing ion permeation activity.

**Investigation of the Channel Size by the Hill Equation.** As written above, Hill analysis of Figure 7d suggests that the working channel is a tetrameric assembly of **1**. Furthermore, the discontinuous conductivity observed under the dilute conditions (Figure 4) indicates that the channel has a dynamic feature undergoing opening/closing motions. Taking

into account the folded conformation of **1** in a liposomal membrane to give a plate-like architecture, together with the above-mentioned experimental results, we reconsidered a plausible model of the channel formation by **1** as illustrated in Figure 8. This model represents the self-assembly of four

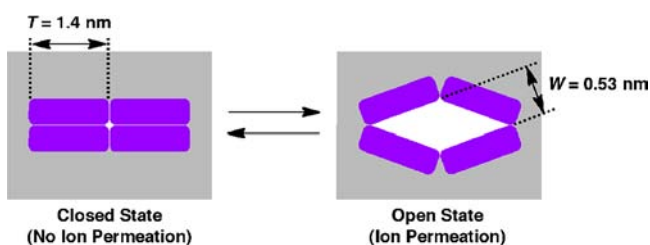


**Figure 8.** Plausible model of the supramolecular channel of **1** (blue rectangles) embedded in a liposomal membrane (gray area). Tetrameric assembly of **1** undergoes opening (left to right) and closing (right to left) of an ion channel in a liposomal membrane by thermal fluctuation. On the basis of the molecular mechanics calculation, the thickness,  $T$ , of **1** adopting folded conformation is estimated to be 1.4 nm. The Hille equation, assuming a rhombic pore, derives the width,  $W$ , between the facing molecules to be 0.53 nm.

molecules of **1** to form a rhombic channel, where the geometry of the molecules changes between the closed and the open states. In this model, the shape of the pore is assumed to be rhombic. Accordingly, we evaluated the pore size using the Hille equation,<sup>1,31</sup> taking into account the rhombic cross section of the channel made by **1**, as follows.

The Hille equation<sup>1,31</sup> predicts the maximum conductance  $g$  for a pore with a specific size, which consists of two terms, the standard expression for the resistance of a body of length  $L$  and uniform cross-sectional area  $S$ , and the access resistance at the two mouths of the pore,<sup>32</sup> as shown in eq 1,

$$\frac{1}{g} = \frac{\rho L}{S} + \frac{\varepsilon \rho}{C} + \frac{\varepsilon \rho}{C} \quad (1)$$

where  $\rho$ ,  $\varepsilon$ , and  $C$  are the resistivity and the permittivity of the solution and the capacitance, respectively. The cross section of the channel in our model is rhombic, and the corresponding capacitance can be estimated as below,<sup>33</sup>

$$C = c_f \varepsilon (4\pi S)^{1/2} = 3.289 \varepsilon S^{1/2} \quad (2)$$

where  $c_f$  is the shape factor of a rhombic disk and approximated to be 0.928. Here  $S$  can be represented as below,

$$S = TW \quad (3)$$

where  $T$  and  $W$  are the thickness of **1** adopting the folded conformation and the width between the facing molecules in the rhombic channel, respectively (Figure 8). By solving the eqs 1 and 2 with the experimentally obtained values and known parameters ( $g = 70$  pS,  $\rho = 2.35 \Omega \text{ m}$ ,  $L = 3.5$  nm) including the Sansom's correction factor,<sup>1,31</sup>  $S$  is estimated to be  $0.76 \text{ nm}^2$ . Here, on the basis of the molecular mechanics calculation of **1**,  $T$  is estimated to be 1.4 nm. Hence, eq 3 gives the value of  $W$  as 0.53 nm (Figure 8). Interestingly, the value of this width is very close to that of the diameter (0.54 nm) of the ion channel reported by Kim and co-workers,<sup>7a</sup> demonstrating the cation selectivity following the Eisenman sequence, XI. They suggest that the interaction between cations and the  $\pi$  system of their channel plays an important role in the ion transport.

## CONCLUSION

A multiblock amphiphilic molecule **1** having alternating sequence of hydrophilic and hydrophobic units, adopts a multipass transmembrane-like structure in a liposomal membrane and assembles to form a nanopore to allow for permeation of ions through the membrane. This function is specific for a molecule, which is able to adopt a panel-like folded structure through intramolecular  $\pi$ - $\pi$  stacks of the hydrophobic moieties. Thus, it is clearly demonstrated that the hierarchical construction of higher-order structures is essential for operating such protein-like functions. The present results should be an important step toward a rational design of programmable and functional molecular organisms beyond a molecule.

## EXPERIMENTAL SECTION

**Methods.**  $^1\text{H}$  nuclear magnetic resonance (NMR) spectra were recorded on a Fourier-transform NMR JNM-LA400 spectrometer (400 MHz, JEOL, Tokyo, Japan) or a Fourier-transform NMR AVANCE III 500 (500 MHz, Bruker BioSpin, Rheinstetten, Germany), where the chemical shifts were determined with respect to tetramethylsilane (TMS) or a residual nondeuterated solvent as an internal standard. Matrix-assisted laser desorption/ionization time-of-flight mass (MALDI-TOF MS) spectrometry was performed in reflector mode with gentisic acid (GA) as a matrix on a REFLEX III spectrometer (Bruker Daltonics, Bremen, Germany). UV-vis spectra were recorded on a V-530 UV-vis spectrophotometer (JASCO, Tokyo, Japan). Fluorescence spectra were recorded on an FP-6500 spectrophotometer (JASCO, Tokyo, Japan). Dynamic light scattering (DLS) was performed with a fiber-optical dynamic light-scattering spectrophotometer FDLS-3000 (Otsuka Electronics, Tokyo, Japan) and analyzed with the CONTIN algorithm. Phase contrast microscopy was performed with a BX-51 microscope (Olympus, Tokyo, Japan) using Olympus Immersion Oil Type F, where Olympus UPLFLN 100XO2PH (magnification: 100 $\times$ ) was attached as the objective lens.

**Reagents.** 1,2-Dioleoyl-*sn*-glycero-3-phosphocholine (DOPC), 1-palmitoyl-2-stearoyl (5-doxyl)-*sn*-glycero-3-phosphocholine (5-doxyl PC), 1-palmitoyl-2-stearoyl (12-doxyl)-*sn*-glycero-3-phosphocholine (12-doxyl PC), and 1-palmitoyl-2-stearoyl (16-doxyl)-*sn*-glycero-3-phosphocholine (16-doxyl PC) were purchased from Avanti Polar Lipids (Alabaster, AL). 8-Hydroxypyrene-1,3,6-trisulfonic acid (HPTS) was purchased from Tokyo Chemical Industry (Tokyo, Japan). Sucrose, LiOH, NaOH, KOH, CsOH, Pd/C (10% Pd), and Triton X-100 were purchased from Nacalai Tesque (Kyoto, Japan). RbOH was purchased from Strem Chemicals (Newburyport, MA). These commercial reagents were used without further purification. Deionized water (filtered through a 0.22  $\mu\text{m}$  membrane filter, >18.2  $\text{M}\Omega \text{ cm}$ ) was purified in a Milli-Q system of Millipore.

**Synthesis of 3.** To a THF (80 mL) suspension of **1** (30 mg, 9.47  $\mu\text{mol}$ ) in an autoclave was added Pd/C (3.0 mg, 2.82  $\mu\text{mol}$  of Pd) and  $\text{H}_2$  (0.80 MPa), and the resulting mixture was heated to 50  $^\circ\text{C}$ . After being stirred for 20 h, the mixture was filtrated through Celite and evaporated to allow isolation of **3** in 82% yield (25 mg, 7.81  $\mu\text{mol}$ ) as off-white solids.  $^1\text{H}$  NMR (400 MHz,  $\text{CDCl}_3$  containing 0.03% TMS, 22  $^\circ\text{C}$ ):  $\delta$  7.79 (s, 2H), 7.46–7.36 (m, 16H), 7.18 (s, 6H), 7.09–7.06 (m, 16H), 6.90–6.88 (m, 16H), 6.69 (s, 3H), 5.38–5.30 (m, 8H), 4.12 (s, 32H), 3.88–3.61 (m, 124H) ppm; MALDI-TOF MS (gentisic acid, positive mode):  $m/z$ : calculated for  $\text{C}_{179}\text{H}_{228}\text{N}_6\text{O}_{46}$ : 3242.53; found: 3242.63 [ $\text{M} + 2\text{Na} - \text{H}$ ] $^+$ .

**Giant Unilamellar Vesicles Preparation.** A typical procedure is as follows. A  $\text{CHCl}_3/\text{MeOH}$  (2/1, v/v) solution of DOPC (2.0 mM, 20  $\mu\text{L}$ ) and a THF solution of **1** or **2** (24  $\mu\text{M}$ , **1**: 43  $\mu\text{L}$  or **2**: 171  $\mu\text{L}$ ) were mixed in a glass tube, and the resulting mixture was gently dried under  $\text{N}_2$  flow to produce a thin lipid film. The film was subsequently dried under vacuum for 3 h and hydrated overnight with sucrose aq (0.20 M, 200  $\mu\text{L}$ ) at 37  $^\circ\text{C}$ . The final DOPC concentration was 0.20 mM.

**Large Unilamellar Vesicles Preparation.** A typical procedure to prepare LUVs•1–3•HPTS is as follows. A CHCl<sub>3</sub> solution of DOPC (2.0 mM, 120 μL) and a THF solution of 1–3 (24 μM, 1 and 3: 120 μL or 2: 480 μL) were mixed in a glass tube, and the resulting mixture was evaporated at 25 °C under reduced pressure to produce a thin lipid film. The film was subsequently dried overnight under vacuum, hydrated with HEPES buffer (20 mM, containing 50 mM KCl, pH 7.1, 2.4 mL) containing 30 μM HPTS, followed by freezing and thawing (five times), and then sonication for 30 min. Sonication was carried out under N<sub>2</sub> at 0–5 °C using an ultrasound bath (USK-4R, 160 W). The obtained suspension was dialyzed at 4 °C using Spectra/Por Dialysis Membrane (MWCO 3500).

**Fluorescence Depth Quenching.** A CHCl<sub>3</sub>/MeOH (2/1, v/v) solution of phospholipids (DOPC alone or a mixture of DOPC (90 mol %) and 5-, 12-, or 16-doxyl PC (10 mol %); [total PC] = 2.0 mM, 40 μL) and a THF solution of 1 or 2 (24 μM, [1 or 2]/[total PC] = 0.00050: 1.7 μL or [1 or 2]/[total PC] = 0.10: 334 μL) were mixed in a glass tube, and the resulting mixture was gently dried under N<sub>2</sub> flow to produce a thin lipid film. The film was subsequently dried under vacuum for 3 h and hydrated overnight with HEPES buffer (20 mM, containing 50 mM KCl, pH 7.1, 0.40 mL) at 37 °C. The final phospholipid concentration was 0.20 mM.

**Observation of Giant Unilamellar Vesicle Deformation by Osmotic Pressure Gradient.** To a 0.20 M sucrose aqueous suspension of DOPC GUV ([DOPC] = 0.20 mM, 5.0 μL) containing 1 ([1]/[DOPC] = 0.025) or 2 ([2]/[DOPC] = 0.10) was added a mixture of 5.0 mM NaCl and 0.20 M sucrose aq (5.0 μL). The resulting mixture ([DOPC] = 0.10 mM, [NaCl] = 2.5 mM, [sucrose] = 0.20 M) was put into a cylinder hollow (i.d. 6 mm, 0.2 mm thick) in a silicon film placed on a glass slide. Soon after the addition of a mixture of 5.0 mM NaCl and 0.20 M sucrose aq, the sample was covered by a cover glass, and phase contrast microscopic observation was started within 5 s. Recording of the images was conducted by a WAT-120N+ CCD camera (Watec, Yamagata, Japan) and an RD-R100 DVD recorder (Toshiba, Tokyo, Japan). All the processes were carried out at 20 °C.

**Evaluation of Bending Elastic Moduli by Micropipet Aspiration.** To estimate the bending elastic moduli of GUVs, we adopted a micropipet aspiration technique.<sup>17c,22a</sup> GUVs were prepared in sucrose aq (0.20 M). An aliquot of the liposome suspension (10 μL) was then mixed with glucose aq (0.20 M, 290 μL) to enhance the image contrast of GUVs under an inverted differential interference contrast (DIC) microscopic observation due to the difference in the refractive indices of the internal and external solutions of the GUVs. A single GUV with a diameter of 20–50 μm was aspirated into a CustomTip type 1 glass micropipet (i.d.: 10 μm, Eppendorf, Hamburg, Germany) using an MN-151 micromanipulator (Narishige, Tokyo, Japan) and a CellTram Vario microinjector (Eppendorf, Hamburg, Germany) set on a TE2000 inverted DIC microscope (Nikon, Tokyo, Japan). Micropipet aspiration was used to pressurize the GUV and stretch the bilayer to rupture. The external aspiration pressure was increased until the GUV was deformed to a tight shape that was recorded using a CCD camera. The pipet and the vesicle diameters, the aspiration length, and the applied aspiration pressure values were recorded to calculate the bending elastic moduli as described in the Supporting Information.

**Conductance Measurement.** Ion channel current recordings of 1 and 2 were conducted as follows. A planar lipid bilayer was prepared by the reported procedure.<sup>34</sup> A mixture of DOPC (12.7 mM) and 1 or 2 (10 nM or 1.0 pM) in *n*-decane was painted on an orifice (*d* = 150 μm), which was sandwiched by two chambers containing HEPES buffer (20 mM HEPES, 50 mM KCl, pH 7.5, 0.30 mL each). Current was measured with a CEZ2400 amplifier (Nihon Kohden, Tokyo, Japan) and stored on a computer using a Power Lab (AD instruments, Nagoya, Japan) at a 40 kHz sampling rate. Recordings were filtered at 1 kHz. To monitor the channel current, membrane voltage was applied at 50, 70, and 80 mV. All the current recordings were performed at 20 °C. The single channel *I*–*V* profile was obtained by plotting the single channel current *I* as a function of membrane potential *V*. According to Ohm's law, the pore conductance *g* was evaluated to be 70 pS.

**Fluorescence Measurement.** To a HEPES buffer (1.99 mL, 20 mM, containing 50 mM KCl, pH 7.1) suspension of LUVs•1–3•HPTS ([DOPC] = 0.10 mM, [HPTS] = 30 μM, [1]/[DOPC] = [3]/[DOPC] = 0.012, [2]/[DOPC] = 0.048) was added an aqueous solution of an alkali hydroxide (0.6 M, 10 μL, ΔpH = 0.8) by a syringe in the dark at 20 °C. Fluorescence intensity of HPTS at 510 nm (excitation at 460 nm) was monitored as a function of time until addition of 1.2% Triton X-100 (40 μL) at 100 s. Relative fluorescence intensity of HPTS entrapped in LUVs in response to the pH enhancement was evaluated by the equation of  $I = (I_t - I_0)/(I_{lyzed} - I_0)$ , where *I*<sub>0</sub>, *I*<sub>*t*</sub>, and *I*<sub>lyzed</sub> represent the fluorescence intensities before addition of an alkali hydroxide, at *t* seconds after addition of an alkali hydroxide, and after lysis by the addition of 1% Triton X-100, respectively.

## ■ ASSOCIATED CONTENT

### ● Supporting Information

Conductance recordings, time course fluorescence measurements, calculation of bending elastic moduli, and videos of phase contrast microscopic observations of DOPC GUVs containing 1 ([1]/[DOPC] = 0.025) and 2 ([2]/[DOPC] = 0.10) in 0.20 M sucrose aqueous solution under exposure to osmotic pressure (2.5 mM NaCl). This material is available free of charge via the Internet at <http://pubs.acs.org>.

## ■ AUTHOR INFORMATION

### Corresponding Author

kinbara@tagen.tohoku.ac.jp

### Notes

The authors declare no competing financial interest.

## ■ ACKNOWLEDGMENTS

We thank Prof. M. Shimomura (Tohoku University) and Dr. T. Higuchi (Tohoku University) for assistances in DLS measurements. We also thank Ms. Y. Kishimoto and Ms. R. Sugimoto for their support in preparation and microscopy of liposomes. This work was partially supported by the Ministry of Education, Culture, Sports, Science and Technology in Japan (MEXT), Grants-in-Aid for Young Scientists S (21675003), Scientific Research on Innovative Areas “Spying minority in biological phenomena” (No.3306), (23115003), and the Management Expenses Grants for National Universities Corporations to K.K. and Noguchi Foundation to T.M.

## ■ REFERENCES

- (1) Hille, B. *Ion Channels of Excitable Membranes*, 3rd ed.; Sinauer Associates: Sunderland, MA, 2001.
- (2) Synthetic ion receptors to transport ions across the lipid bilayer membrane have also been developed. (a) Busschaert, N.; Kirby, I. L.; Young, S.; Coles, S. J.; Horton, P. N.; Light, M. E.; Gale, P. A. *Angew. Chem., Int. Ed.* **2012**, *51*, 4426–4430. (b) Bahmanjah, S.; Zhang, N.; Davis, J. T. *Chem. Commun.* **2012**, *48*, 4432–4434. (c) Busschaert, N.; Wenzel, M.; Light, M. E.; Iglesias-Hernández, P.; Pérez-Tomás, R.; Gale, P. A. *J. Am. Chem. Soc.* **2011**, *133*, 14136–14148. (d) Hussain, S.; Brotherhood, P. R.; Judd, L. W.; Davis, A. P. *J. Am. Chem. Soc.* **2011**, *133*, 1614–1617. (e) De Cola, C.; Licen, S.; Comegna, D.; Cafaro, E.; Bifulco, G.; Izzo, I.; Tecilla, P.; De Riccardis, F. *Org. Biomol. Chem.* **2009**, *7*, 2851–2854. (f) Davis, J. T.; Gale, P. A.; Okunola, O. A.; Prados, P.; Iglesias-Sánchez, J. C.; Torroba, T.; Quesada, R. *Nature Chem.* **2009**, *1*, 138–144.
- (3) Si, W.; Chen, L.; Hu, X.-B.; Tang, G.; Chen, Z.; Hou, J.-L.; Li, Z.-T. *Angew. Chem., Int. Ed.* **2011**, *50*, 12564–12568.
- (4) Weiss, L. A.; Sakai, N.; Ghebremariam, B.; Ni, C.; Matile, S. *J. Am. Chem. Soc.* **1997**, *119*, 12142–12149.

- (5) (a) Zhou, X.; Liu, G.; Yamato, K.; Shen, Y.; Cheng, R.; Wei, X.; Bai, W.; Gao, Y.; Li, H.; Liu, Y.; Liu, F.; Czajkowsky, D. M.; Wang, J.; Dabney, M. J.; Cai, Z.; Hu, J.; Bright, F. V.; He, L.; Zeng, X. C.; Shao, Z.; Gong, B. *Nat. Commun.* **2012**, *3*, 949. (b) Hennig, A.; Fischer, L.; Guichard, G.; Matile, S. *J. Am. Chem. Soc.* **2009**, *131*, 16889–16895. (c) Cazacu, A.; Legrand, Y.-M.; Pasc, A.; Nasr, G.; van der Lee, A.; Mahon, E.; Barboiu, M. *Proc. Natl. Acad. Sci. U.S.A.* **2009**, *106*, 8117–8122. (d) Biron, E.; Otis, F.; Meillon, J.-C.; Robitaille, M.; Lamothe, J.; van Hove, P.; Cormier, M.-E.; Voyer, N. *Bioorg. Med. Chem.* **2004**, *12*, 1279–1290. (e) Ghadiri, M. R.; Granja, J. R.; Buehler, L. K. *Nature* **1994**, *369*, 301–304. (f) Roks, M. F. M.; Nolte, R. J. M. *Macromolecules* **1992**, *25*, 5398–5407. (g) Tabushi, I.; Kuroda, Y.; Yokota, K. *Tetrahedron Lett.* **1982**, *23*, 4601–4604.
- (6) (a) Moszynski, J. M.; Fyles, T. M. *Org. Biomol. Chem.* **2011**, *9*, 7468–7475. (b) Wilson, C. P.; Boglio, C.; Ma, L.; Cockroft, S. L.; Webb, S. J. *Chem.—Eur. J.* **2011**, *17*, 3465–3473.
- (7) (a) Jung, M.; Kim, H.; Baek, K.; Kim, K. *Angew. Chem., Int. Ed.* **2008**, *47*, 5755–5757. (b) Li, X.; Shen, B.; Yao, X.-Q.; Yang, D. *J. Am. Chem. Soc.* **2007**, *129*, 7264–7265. (c) Schrey, A.; Vescovi, A.; Knoll, A.; Rickert, C.; Koert, U. *Angew. Chem., Int. Ed.* **2000**, *39*, 900–902. (d) Murillo, O.; Suzuki, L.; Abel, E.; Murray, C. L.; Meadows, E. S.; Jin, T.; Gokel, G. W. *J. Am. Chem. Soc.* **1997**, *119*, 5540–5549. (e) Kobuke, Y.; Ueda, K.; Sokabe, M. *J. Am. Chem. Soc.* **1992**, *114*, 7618–7622. (f) Fuhrhop, J.-H.; Liman, U.; Koesling, V. *J. Am. Chem. Soc.* **1988**, *110*, 6840–6845. (g) Lear, J. D.; Wasserman, Z. R.; De Grado, W. F. *Science* **1988**, *240*, 1177–1181.
- (8) (a) Boudreault, P.-L.; Voyer, N. *Org. Biomol. Chem.* **2007**, *5*, 1459–1465. (b) Vandenburg, Y. R.; Smith, B. D.; Biron, E.; Voyer, N. *Chem. Commun.* **2002**, 1694–1695.
- (9) Tanaka, H.; Litvinchuk, S.; Tran, D.-H.; Bollot, G.; Mareda, J.; Sakai, N.; Matile, S. *J. Am. Chem. Soc.* **2006**, *128*, 16000–16001.
- (10) (a) Cho, H.; Widanapathirana, L.; Zhao, Y. *J. Am. Chem. Soc.* **2011**, *133*, 141–147. (b) Yang, L.; Gordon, V. D.; Mishra, A.; Som, A.; Purdy, K. R.; Davis, M. A.; Tew, G. N.; Wong, G. C. L. *J. Am. Chem. Soc.* **2007**, *129*, 12141–12147. (c) Litvinchuk, S.; Bollot, G.; Mareda, J.; Som, A.; Ronan, D.; Shah, M. R.; Perrottet, P.; Sakai, N.; Matile, S. *J. Am. Chem. Soc.* **2004**, *126*, 10067–10075.
- (11) (a) Otis, F.; Racine-Berthiaume, C.; Voyer, N. *J. Am. Chem. Soc.* **2011**, *133*, 6481–6483. (b) *Handbook of Cell-Penetrating Peptides*; Langel, Ü, Ed.; CRC Press: Boca Raton, FL, 2007.
- (12) (a) Boudreault, P.-L.; Arseneault, M.; Otis, F.; Voyer, N. *Chem. Commun.* **2008**, 2118–2120. (b) Leevy, W. M.; Huettner, J. E.; Pajewski, R.; Schlesinger, P. H.; Gokel, G. W. *J. Am. Chem. Soc.* **2004**, *126*, 15747–15753.
- (13) Petsko, G. A.; Ringe, D. *Protein Structure and Function*; New Science Press: London, 2004.
- (14) (a) Juwarker, H.; Suk, J.; Jeong, K.-S. *Chem. Soc. Rev.* **2009**, *38*, 3316–3325. (b) Saraogi, I.; Hamilton, A. D. *Chem. Soc. Rev.* **2009**, *38*, 1726–1743. (c) Bao, C.; Kauffmann, B.; Gan, Q.; Srinivas, K.; Jiang, H.; Huc, I. *Angew. Chem., Int. Ed.* **2008**, *47*, 4153–4156. (d) Horne, W. S.; Gellman, S. H. *Acc. Chem. Res.* **2008**, *41*, 1399–1408. (e) Horne, W. S.; Price, J. L.; Keck, J. L.; Gellman, S. H. *J. Am. Chem. Soc.* **2007**, *129*, 4178–4180. (f) Daniels, D. S.; Petersson, E. J.; Qiu, J. X.; Schepartz, A. *J. Am. Chem. Soc.* **2007**, *129*, 1532–1533. (g) *Foldamers: Structure, Properties, and Applications*; Hecht, S., Huc, I., Eds.; Wiley-VCH: Weinheim, 2007. (h) Goto, H.; Katagiri, H.; Furusho, Y.; Yashima, E. *J. Am. Chem. Soc.* **2006**, *128*, 7176–7178. (i) Sinkeldam, R. W.; van Houtem, M. H. C. J.; Pieterse, K.; Vekemans, J. A. J. M.; Meijer, E. W. *Chem.—Eur. J.* **2006**, *12*, 6129–6137. (j) Jones, T. V.; Slutsky, M. M.; Laos, R.; de Greef, T. F. A.; Tew, G. N. *J. Am. Chem. Soc.* **2005**, *127*, 17235–17240. (k) Abe, H.; Masuda, N.; Waki, M.; Inouye, M. *J. Am. Chem. Soc.* **2005**, *127*, 16189–16196. (l) Ghosh, S.; Ramakrishnan, S. *Angew. Chem., Int. Ed.* **2004**, *43*, 3264–3268. (m) Wang, W.; Li, L.-S.; Helms, G.; Zhou, H.-H.; Li, A. D. Q. *J. Am. Chem. Soc.* **2001**, *125*, 1120–1121. (n) Nakano, T.; Okamoto, Y. *Chem. Rev.* **2001**, *101*, 4013–4038. (o) Hill, D. J.; Mio, M. J.; Prince, R. B.; Hughes, T. S.; Moore, J. S. *Chem. Rev.* **2001**, *101*, 3893–4011. (p) Berl, V.; Huc, I.; Khoury, R. G.; Krische, M. J.; Lehn, J.-M. *Nature* **2000**, *407*, 720–723. (q) Gellman, S. H. *Acc. Chem. Res.* **1998**, *31*, 173–180. (r) Nelson, J. C.; Saven, J. G.; Moore, J. S.; Wolynes, P. G. *Science* **1997**, *277*, 1793–1796. (s) Lokey, R. S.; Iverson, B. L. *Nature* **1995**, *375*, 303–305.
- (15) Muraoka, T.; Shima, T.; Hamada, T.; Morita, M.; Takagi, M.; Kinbara, K. *Chem. Commun.* **2011**, *47*, 194–196.
- (16) Levitus, M.; Schmieder, K.; Ricks, H.; Shimizu, K. D.; Bunz, U. H. F.; Garcia-Garibay, M. A. *J. Am. Chem. Soc.* **2001**, *123*, 4259–4265.
- (17) (a) Hamada, T.; Sugimoto, R.; Vestergaard, M.; Nagasaki, T.; Takagi, M. *J. Am. Chem. Soc.* **2010**, *132*, 10528–10532. (b) Morita, M.; Vestergaard, M.; Hamada, T.; Takagi, M. *Biophys. Chem.* **2010**, *147*, 81–86. (c) Ishii, K.; Hamada, T.; Hatakeyama, M.; Sugimoto, R.; Nagasaki, T.; Takagi, M. *ChemBioChem* **2009**, *10*, 251–256. (d) Hamada, T.; Miura, Y.; Ishii, K.; Araki, S.; Yoshikawa, K.; Vestergaard, M.; Takagi, M. *J. Phys. Chem. B* **2007**, *111*, 10853–10857.
- (18) (a) Weiss, L. A.; Sakai, N.; Ghebremariam, B.; Ni, C.; Matile, S. *J. Am. Chem. Soc.* **1997**, *119*, 12142–12149. (b) Ren, J.; Lew, S.; Wang, Z.; London, E. *Biochemistry* **1997**, *36*, 10213–10220. (c) Ladokhin, A. S. *Methods Enzymol.* **1997**, *278*, 462–473.
- (19) On the basis of a molecular modeling study, the spin probes of 5-, 12-, and 16-doxyl PCs are found to lie 1.2, 0.6, and 0.2 nm away from the middle of a bilayer membrane, respectively.
- (20) (a) Yanagisawa, M.; Imai, M.; Taniguchi, T. *Phys. Rev. Lett.* **2008**, *100*, 148102. (b) Hamada, T.; Miura, Y.; Ishii, K.; Araki, S.; Yoshikawa, K.; Vestergaard, M.; Takagi, M. *J. Phys. Chem. B* **2007**, *111*, 10853–10857. (c) Hotani, H. *J. Mol. Biol.* **1984**, *178*, 113–120.
- (21) It is confirmed that no fluctuating vesicle was present before adding NaCl.
- (22) (a) Rawicz, W.; Olbrich, K. C.; McIntosh, T.; Needham, D.; Evans, E. *Biophys. J.* **2000**, *79*, 328–339. (b) Evans, E.; Rawicz, W. *Phys. Rev. Lett.* **1990**, *64*, 2094–2097.
- (23) Bending elastic modulus of GUVs•1 was  $B_{\text{GUVs}\bullet 1} = 2.7 \times 10^{-20}$  J, which is comparable to  $B_{\text{GUVs}\bullet 2}$ .
- (24) Even in the case of molecules such as cholesterol that are favorable for the flip–flop motion, the rate is 10-s order. Lasic, D. D., *Liposomes: From Physics to Applications*; Elsevier: Amsterdam, 1993.
- (25) Hessel, E.; Herrmann, A.; Müller, P.; Schnerkamp, P. P. M.; Hofmann, K.-P. *Eur. J. Biochem.* **2000**, *267*, 1473–1483.
- (26) One hundred and twenty-six molecules of 1 are evaluated to be involved in the orifice in this condition; see Lewis, B. A.; Excelman, D. M. *J. Mol. Biol.* **1983**, *166*, 211–217.
- (27) (a) Clement, N. R.; Gould, J. M. *Biochemistry* **1981**, *20*, 1534–1538. (b) Kano, K.; Fendler, J. H. *Biochim. Biophys. Acta* **1978**, *509*, 289–299.
- (28) Eisenman, G.; Horn, R. *J. Membr. Biol.* **1983**, *76*, 197–225.
- (29) (a) Tedesco, M. M.; Ghebremariam, B.; Sakai, N.; Matile, S. *Angew. Chem., Int. Ed.* **1999**, *38*, 540–543. (b) Kumpf, R. A.; Dougherty, D. A. *Science* **1993**, *261*, 1708–1710.
- (30) Hill, A. V. *Biochem. J.* **1913**, *7*, 471–480.
- (31) Smart, O. S.; Breed, J.; Smith, G. R.; Sansom, M. S. P. *Biophys. J.* **1997**, *72*, 1109–1126.
- (32) Hall, J. E. *J. Gen. Physiol.* **1975**, *66*, 531–532.
- (33) Chow, Y. L.; Yovanovich, M. M. *J. Appl. Phys.* **1982**, *53*, 8470–8475.
- (34) Tabata, K. V.; Sato, K.; Ide, T.; Nishizaka, T.; Nakano, A.; Noji, H. *EMBO J.* **2009**, *28*, 3279–3289.